Journal of Environmental Management 248 (2019) 109310

Contents lists available at ScienceDirect

Journal of Environmental Management

journal homepage: www.elsevier.com/locate/jenvman

Research article

Bioelectricity generation from the decolorization of reactive blue 19 by using microbial fuel cell

Haitao Wang[a], Qiang Wang[a], Xiang Li[b], Yuanpeng Wang[a], Pu Jin[a], Yi Zheng[b,*], Jiale Huang[a,**], Qingbiao Li[a,c]

[a] Department of Chemical and Biochemical Engineering, College of Chemistry and Chemical Engineering, Xiamen University, No. 422 Siming South Road, Xiamen, 361005, PR China
[b] Department of Grain Science and Industry, Kansas State University, 101C BIVAP, 1980 Kimball Avenue, Manhattan, KS, 66506, USA
[c] College of Food and Biological Engineering, Jimei University, Xiamen, 361021, PR China

ARTICLE INFO

Keywords:
Microbial fuel cell
Anthraquinone dye
Decolorization
Bioelectricity
High-throughput 16S rRNA
Microbial community structure

ABSTRACT

Microbial fuel cell (MFC) was compared to conventional biological techniques for decolorization of anthraquinone dye, reactive blue 19 (RB19) with simultaneous electricity generation. With 50 mg/L of RB19 in the anode chamber as a fuel, the MFC achieved 89% decolorization efficiency of RB19 within 48 h, compared with 51 and 55% decolorization efficiency achieved by aerobic and anaerobic techniques, respectively. The cyclic voltammetry results showed that RB19 could promote the electron transfer and redox reaction on the surface of anode. The RB19 decolorization process can be described by first-order kinetics, and the decolorization rate decreased with the increase of RB19 concentration. The high-throughput 16S rRNA sequencing analysis indicated significant microbial community shift in the MFC. At phylum level, the majority of sequences belong to *Proteobacteria*, accounting from 23 to 84% of the total reads in each bacterium community. At genus level, the MFC contained two types of microorganisms in general such as electrochemically active and decolorization bacteria. Overall, MFC is an effective method for anthraquinone dye treatment with simultaneous energy recovery. The 16S rRNA revealed that there were two major functioning microbial communities in the MFC such as electricity-producing and RB19-degrading bacteria which synergistically worked on RB19 degradation.

1. Introduction

It is well known that the dye industry generates a large amount of wastewater during dyeing, printing and finishing processes. About 10–15% of the dyes ends up in the wastewater which is highly toxic to human beings and animals (Basturk and Karatas, 2014; Ning et al., 2015). The dye-containing wastewater has complex characteristics, such as deep chromaticity, low light penetration, complicated composition, and severe environmental pollution (Buscio et al., 2015; Shamsnejati et al., 2015). Therefore, effective treatment of dyes is imperative to eliminate the potential hazard of dye pollutants to the receiving water bodies.

Anthraquinone dyes are the second largest class of dyes after the azo dyes (Basturk and Karatas, 2014). They possess stable structure of polycyclic aromatic rings and have extensive applications (Basturk and Karatas, 2014; Jenmao and Dyihwa, 2009). Anthraquinone has become one of major dye pollutants in industrial wastewater. Anthraquinone dye wastewater is characterized by high colority, slow decolorization, complex composition, and low biochemical availability (biochemical oxygen demand (BOD)/chemical oxygen demand (COD) < 0.1), strong toxicity, etc. The World Health Organization's International Agency for Research on Cancer released a preliminary list of carcinogens where anthraquinones is in the 2B list of carcinogens (https://monographs.iarc.fr/list-of-classifications-volumes/). During dyeing process, about 50% of anthraquinone dye is eventually discharged to the wastewater, leading to high chroma and low biodegradability of the wastewater (O'Neill et al., 2015). Compared with azo dyes, biological degradation of anthraquinone dyes are more challenging because the anthraquinone structure (i.e., chromophoric groups) is stabilized by resonance while the degradation intermediates (e.g., aromatic amine) of anthraquinone dyes are usually toxic to microorganisms and carcinogenic (Ge et al., 2015).

Physicochemical methods, such as advanced oxidation (Asghar et al., 2015a, 2015b), electrochemical (Brillas and Martínez-Huitle,

* Corresponding author.
** Corresponding author.
E-mail addresses: yzheng@ksu.edu (Y. Zheng), cola@xmu.edu.cn (J. Huang).

https://doi.org/10.1016/j.jenvman.2019.109310
Received 25 March 2019; Received in revised form 5 July 2019; Accepted 24 July 2019
Available online 31 July 2019
0301-4797/

2015), photocatalytic oxidation (Habibi et al., 2005), ultrasounds (Wang et al., 2008), Fenton oxidation (Sun et al., 2007), UV/H_2O_2 (Bali et al., 2004), and ozonation (Soares et al., 2006) have been broadly used in the decolorization of anthraquinone dye. Although the physicochemical methods are effective for the degradation of anthraquinone dyes, they have disadvantages of high cost and incomplete mineralization (i.e., anthraquinone can't be completely degraded into small molecules, such as CO_2 and H_2O). Alternatively, biological treatment including activated sludge (Santos and Boaventura, 2015; Beydilli et al., 2000), fungi and algae (Imran et al., 2015) are expected to be a relatively more cost-efficient to remove dyes from wastewater. Although some commonly studied decolorizing microorganisms such as *Aspergillus*, *Pseudomonas*, *Shewanella*, *Rhizobium*, and *Radiobacter* are often employed in the decolorization of dye-containing wastewater, they are unable to completely degrade anthraquinone dyes (Ge et al., 2015). The degradation efficiency of anthraquinone dyes mainly depends on the microbial capacity to remove chromogenic groups. Because of their high solubility in water, anthraquinone dyes poorly adsorb onto biomass so that they can't be readily degraded under typical aerobic conditions. The key step in biodegradation of anthraquinone dyes is the removal of chromogenic groups from the aromatic nucleus through either reductive or hydrolytic enzymes of anaerobic microorganisms. Although most anaerobic microorganisms have enzymes necessary for aromatic ring degradation, they have limited capacity of removing chromogenic groups. Fontenot et al. conducted laboratory experiments with mixed methanogenic culture under the initial concentration of RB19 more than 300 mg/L, which resulted in complete inhibition of methanogenesis (Fontenot et al., 2002). Therefore, research is still needed to find effective approaches for anthraquinone dye treatment.

As a new type of biological approach, microbial fuel cell (MFC) has attracted more and more research interest in wastewater treatment because they can treat wastewater and simultaneously transform the chemical energy of organic matters in the wastewater directly into electricity via the catalysis of electroactive microorganisms (An et al., 2016; Feng et al., 2015; Logan et al., 2015; Penteado et al., 2016). Also, the MFC could be operated under mild conditions with little energy input. However, most previous work has focused on the application of MFC on the degradation of azo dyes. For instance, Jian et al. (2009) and Sun et al. (2011) used the MFC for simultaneous decolorization and degradation of azo dyes. Fang et al. (Zhou et al., 2015) treated reactive brilliant red wastewater with MFC and achieved decoloring rate of 93% with the power density of 619 mW/m^2 with the hydraulic retention time being 3 days. Although anthraquinone is a common dye, little research has been done on the treatment of anthraquinone dyes by using MFC.

Therefore, this research aimed at examining the reactive blue 19 (RB19) (as a representative anthraquinone dye) decolorization by using MFC, which was carried out in the anode chamber of a two-chamber MFC. At the anode, microorganisms are essential for electricity production because they are able to catalyze the oxidation of organic co-substrate (e.g., acetate and glucose) and transfer the produced electrons to the anode which then pass through the external circuit to the cathode, thus generating the current. In the presence of co-substrate, microbial enzyme activity can be enhanced, and the degradation efficiency of non-growth matrix can be improved. Therefore, some organic compounds are usually added into microbial processes as primary energy before they can be degraded such as glucose and acetate. This kind of material is called exogenous substance or hetero-biomass. Anaerobic sludge with mixed culture was acclimated to anthraquinone dyes and used as an inoculum to the anode chamber because it could perform better than single culture due to the synergistic interactions within the anode communities (Du et al., 2007; Jung and Regan, 2007). As a result, it is necessary to understand the microbial community structure and dominant species in the anode chamber in order to enhance the performance of the MFC for simultaneous decolorization of anthraquinone dyes and bioelectricity generation.

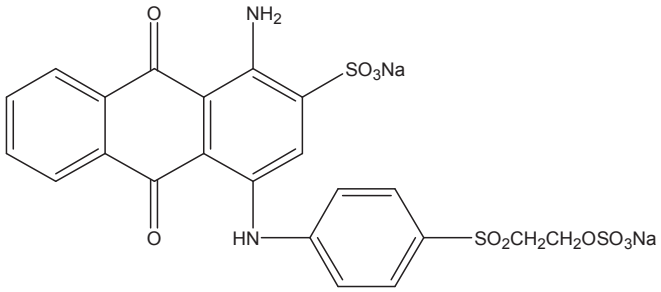

Fig. 1. Molecular formula of RB19.

In addition, the MFC technology was compared with the traditional anaerobic and aerobic processes for RB19 decolorization. The effect of RB19 concentration on the decolorization efficiency was also studied in the range of 50–300 mg/L. To examine the microbial diversity in the anode chamber, the anaerobic inoculum sludge was analyzed for its microbial community before and after the acclimation process by using the high-throughput 16S rRNA sequencing, which was compared with that of the aerobic RB19 treatment process. The results of culture analysis will be useful to advance the decolorization efficiency of RB19 by MFC through culture optimization in the future.

2. Methodology

2.1. Chemicals

A commercial anthraquinone dye, RB19 ($C_{22}H_{16}N_2Na_2O_{11}S_3$, Fig. 1) was provided by Xiamen Hualun Printing & Dyeing Co. Ltd. (Xiamen, China) and used without further purification. All other chemicals purchased from Sinopharm Chemical Reagent Co. Ltd. (Shanghai, China) were analytical grade unless specified, otherwise.

2.2. MFC setup construction and inoculation

The construction of the MFC and working circuit for this study are shown in Fig. 2. The MFC was made from plexiglass and consisted of two 500-mL chambers separated by a cation exchange membrane (Grion 1201, Zhejiang Century Environmental Protection Water Treatment Co., Ltd., Zhejiang, China). Both anode and cathode electrodes were made from carbon felts (5.0 cm × 5.0 cm × 0.5 cm) which encapsulated titanium wire with a diameter of 1 mm. Before used, the carbon felt underwent a series of treatments, including heating in 10% H_2O_2 at 90 °C for 2 h, washing with distilled (DI) water for 2–3 times, heating in 10% H_2O_2 at 90 °C for 1 h, washing with DI water to remove residual H_2O_2, and drying at 60 °C for 1 h, in that order. Anode and cathode electrodes were connected with a copper wire through a 1-kΩ external resistor. A voltmeter was connected in parallel with the resistor to measure the output voltage of the MFC.

In this study, both anaerobic and aerobic sludges were obtained from Xiamen Domestic Sewage Treatment Plant (Xiamen, China) that doesn't receive anthraquinone dye-contaminated wastewater. Anaerobic and aerobic microorganisms were cultured in simulated RB19 wastewater in the two reactors separately. The simulated RB19 wastewater contained (per liter): 3 g of NaCl, 0.191 g of NH_4Cl, 0.44 g of KH_2PO_4, 1.5 g of $NaHCO_3$, 0.1 g of $CaCl_2$, 0.1 g of $MnSO_4{\cdot}H_2O$, 0.1 g of $FeSO_4{\cdot}7H_2O$, 0.1 g of $CoCl_2{\cdot}6H_2O$, 0.1 g of $ZnSO_4{\cdot}7H_2O$, 0.01 g of $CuSO_4{\cdot}5H_2O$, 0.01 g of $AlK(SO_4)_2{\cdot}12H_2O$, and 0.01 g of $Na_2MoO_4{\cdot}2H_2O$. Both NH_4Cl and KH_2PO_4 were added based on the RB19 concentration to achieve the ratio of carbon source, nitrogen source and phosphorus source(C/N/P) to 100:5:1 (Wang et al., 2007). The nutrient ratio in biochemical treatment is determined according to the microbial requirements in sludge. The carbon/nitrogen/phosphorus ratio required by various microorganisms is different, but there is an empirical value for the microbial community of activated sludge, which is 100:5:1

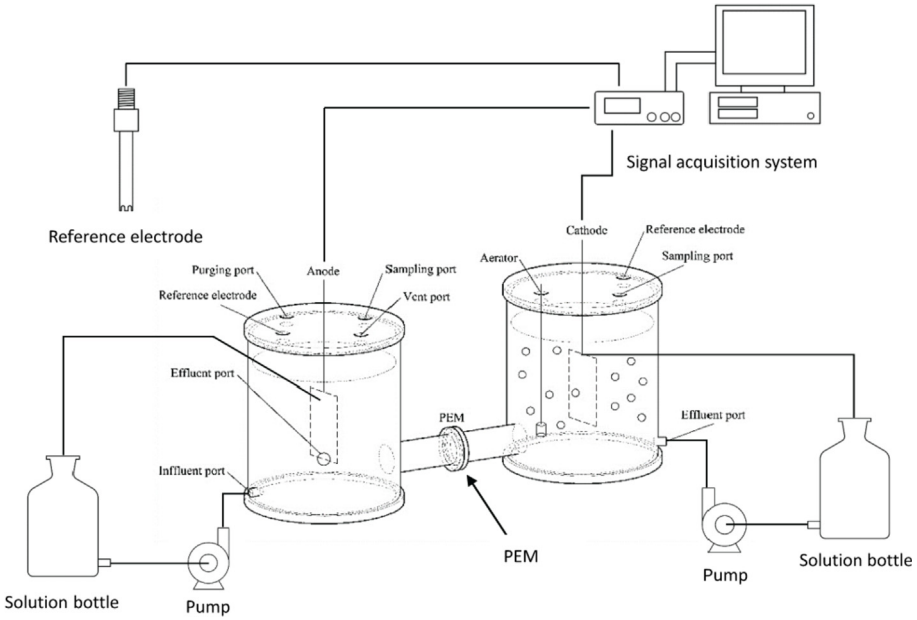

Fig. 2. Schematic of microbial fuel cell setup for decolorization of RB19.

under aerobic conditions and 200:5:1 under anaerobic conditions (Wang et al., 2007). In order to improve the microorganisms' adaptability to the anthraquinone dye wastewater, the RB19 concentration was increased gradually from 50 to 300 mg/L during the acclimation process in about 6 months with glucose as an external carbon source for co-metabolism (Wang et al., 2007). After 20 days of acclimation, the anaerobic and aerobic sludge were added to the MFC pool. The inoculation volume was 500 mL, and the pH was about 7.

2.3. MFC startup and operation

Prior to the decolorization of RB19 in the anode chamber, a mixed culture of electrogenesis microorganisms was inoculated into the anode chamber with the addition of 20 mM sodium acetate to make sure the electrogens worked normally. Once the voltage output was stable, the pre-acclimated anaerobic sludge (from Section 2.2) was inoculated into the anode chamber and the substrate was changed to glucose as the sole carbon source. After 4 weeks, RB19 was then added to the anode chamber while vitamin and mineral solutions (10 mL each) were added into both anode and cathode chambers together with 5.88 g/L of NaCl, 0.10 mg/L of KCl and 0.25 g/L of NH_4Cl. The pHs of both chambers were adjusted to 7.0 using 0.05 M phosphate buffer (PB) (Table 1). The content in the anode chamber was agitated at 600 rpm/min with a magnetic stir. Meanwhile, air was continuously bubbled into the cathode chamber at the flow rate of 300 mL/min. All experiments were carried out at 30 °C.

In the degradation of RB19 in MFC (Fig. 2), four decolorization processes were conducted for comparison including:

Table 1
Media for anode and cathode chambers.

Component	Concentration in anode medium	Concentration in cathode medium
Sodiumacetate	20 mM	–
NH_4Cl	–	1 mol/L
$NaHCO_3$	–	1 g/L
Vitamin	10 mL/L	10 mL/L
Mineral solutions	10 mL/L	10 mL/L
Phosphate buffer (pH7.0)	0.05 M	0.05 M

(1) Degradation of RB19 under aerobic condition using acclimated aerobic sludge with open circuit,
(2) Degradation of RB19 under anaerobic condition using acclimated anaerobic sludge with open circuit,
(3) Degradation of RB19 with close circuit,
(4) Blank control which contained simulated RB19 wastewater only under aseptic condition (open circuit). It was conducted to detect if RB19 was adsorbed by the electrode.

To study the effect of initial concentration on decolorization efficiency in the MFC, a series of RB19 concentrations were created in the anode chamber including 50, 80, 120, 200, and 300 mg/L. During the test, the RB19 concentrations were monitored periodically by measuring the absorbance at 590 nm of wavelength using UV-VIS spectrophotometer (UV310, UNICOM, England) and the decolorization efficiency was calculated versus time to study the RB19 decolorization kinetics.

2.4. Analysis of RB19 degradation and power generation

Power density and polarization curves were obtained for each experiment at the stable condition of the MFC by recording voltage against the external resistance from 25 to 9000 Ω. The open circuit voltage and the respective anodic and cathodic potentials were measured by using an Electrochemical Workstation when the MFC was stable at each specific external resistance.

The current density I (A/m^2) and the power density P (W/m^2) of the system were calculated using the following equations:

$$I = V/(R \times A) \quad (1)$$

$$P = V \times I/A \quad (2)$$

where, I (A/m^2) = current density, P (W/m^2) = power density, V (V) = cell voltage, R (Ω) = external resistance, and A (m^2) = the surface area of the anode carbon felt.

Cyclic voltammetry (CV) was performed by using a potentiostat (CHI660e, Shanghai Chenhua Instrument Co., Ltd., China) which was connected to a computer, with a scan rate of 1–10 mV/s. In the CV experiment, the working electrode potential was ramped linearly versus time like linear sweep voltammetry. CV took the experiment a step further than linear sweep voltammetry which ended when it reached a

set potential. When CV reached a set potential, the working electrode's potential ramp was inverted. This inversion can happen multiple times during a single experiment. The current at the working electrode was plotted versus the applied voltage to give the cyclic voltammogram trace. Voltammograms were recorded by using a conventional three-electrode system consisting of a working electrode (MFC anode with attached bacteria), a reference electrode (calomel electrode) (SCE, Shanghai Chenhua Instrument Co., Ltd., China) and a counter electrode (platinum wire) (Shanghai Chenhua Instrument Co., Ltd., China).

The RB19 degradation was monitored by measuring the absorbance of wastewater at 590 nm with a UV-VIS spectrophotometer (UV310, UNICOM, England). Decolorization efficiency was determined by monitoring the absorbance decrease in the wastewater and calculated according to Eq. (3):

$$\text{Decolorization efficiency} = (A_a - A_b)/A_a \times 100\% \quad (3)$$

where, A_a and A_b are the absorbance of wastewater at 590 nm before and after treatment, respectively. To prepare samples for COD measurement, aliquots of 2 mL were taken periodically and centrifuged at 12,000 rpm for 10 min and the supernatants were collected for COD measurement (Gilcreas, 1995). The pH and dissolved oxygen level were measured with a pH meter (210A, Orion, USA) and a dissolved oxygen meter (SJG-203A, Shanghai Fine Victory Scientific Instrument Co., Ltd., Shanghai, China), respectively. All the reported data were in three biological replicates unless specified, otherwise.

2.5. FTIR analysis

FTIR analysis was conducted on sludge at time 0 and 96 h after the RB19 was added into anode chamber of the MFC to detect whether some of RB19 has been absorbed by the sludge during its biodegradation. The sludge samples were withdrawn from the anode chamber of the MFC and centrifuged. The supernatants were discarded, and the solid pellets were collected and freeze-dried for FTIR analysis (Nicolet 6700, USA). The FTIR spectra were analyzed following the interpretation criteria reported by Skoog et al. (1998).

2.6. Microbial community analysis

The high-throughput 16S rRNA gene sequencing was employed to investigate the change of microbial community structure during the sludge acclimation and MFC treatment. Sludge samples (A1-A5) were used for sequencing including:

A1: original anaerobic sludge
A2: acclimated anaerobic sludge for RB19 decolorization,
A3: acclimated aerobic sludge for RB19 decolorization,
A4: the sludge from the anode chamber of the MFC without the addition of RB19,
A5: the sludge from the anode chamber of the MFC with RB19.

The sequencing work was done by Shanghai Meiji Biotechnique Institution, China. The sludges were sampled and stored under −80 °C until analyzed. Microbial DNA was extracted from 0.5 g sludge sample using the Fast DNA Spin Kit for soil (MP Biomedical, California, USA) according to the manufacturer's protocol. The PCR was performed to amplify the V3–V4 region of the 16S rRNA by following the program: 95 °C for 5 min, 30 cycles at 94 °C for 5 min, 55 °C for 30 s, 72 °C for 30 s, and finally 72 °C for 10 min. The used primers included 5′-ACTC CTACGGGAGGCAGCA-3′ and 5′-GGACTACHVGGGTWTCTAAT-3′, where barcode was an eight-base sequence unique to each sample.

Amplicons were extracted and purified using the AxyPrep DNA Gel Extraction Kit (Axygen Biosciences, Union City, CA, USA) according to the manufacturer's instructions and quantified using QuantiFluor™-ST (Promega, city, state, USA). Purified amplicons were pooled in equimolar and paired-end sequenced (2 × 250) on an Illumina MiSeq platform according to the standard protocols.

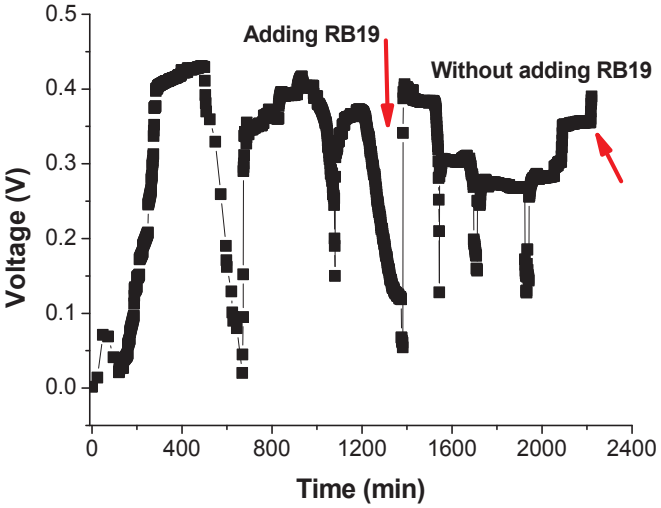

Fig. 3. MFC voltage output during startup stage.

Raw fastq files were demultiplexed and quality-filtered using QIIME (version 1.17) with the following criteria: (i) the 300 bp reads were truncated at any site receiving an average quality score < 20 over a 50 bp sliding window, and the truncated reads that were shorter than 50 bp were discarded; (ii) reads containing ambiguous characters were removed; (iii) only sequences that overlap longer than 10 bp were assembled according to their overlap sequence. Reads which cannot be assembled were discarded. After processing, the reads were assigned to species equivalent operational taxonomic units (OTUs) at ~97% sequence similarity.

3. Results and discussion

3.1. Startup of MFC

The MFC was started with the acclimation of electrogenesis bacteria in the anode chamber in sodium acetate medium with the external resistance of 1 kΩ. At this stage, the spent medium was replaced with fresh one periodically in the anode chamber whenever the voltage decreased to about 50 mV, which was defined as one MFC cycle (Fig. 3). As shown in Fig. 3, the 1st cycle lasted about 700 h during which the voltage showed four distinct phases [i.e., lag phase (0–0.02 V in 100 h), log phase (0.02–0.4 V in 300 h), stationary phase (0.4–0.43 V from 400 to 500 h), and death phase (0.43–0 V from 500 to 600 h)]. Such trend appeared to correspond to a typical four-phase bacterium growth pattern. The span of each cycle decreased significantly to 400 and 300 h for the 2nd and 3rd cycles, respectively. The MFC reached stable status and the voltage exhibited a good reproducibility after three cycles in about 1400 h during acclimation, which meant the MFC startup was successful and ready for wastewater decolorization tests.

At the beginning of decolorization test, 10 mL of pre-acclimated anaerobic sludge was inoculated into the anode chamber together with 50 mg/L of RB19 (the first red arrow in Fig. 3). The MFC voltage increased rapidly from 0.05 to 0.42 V in the presence of RB19 (Fig. 3) because RB19 was a strong electron donor and able to promote the generation of electricity in the MFC. Chen et al. (2013) found that the intermediates of the dye degradation can act as electronic-shuttling mediators to enhance the capabilities of the MFC in both reductive decolorization and bioelectricity generation. However, the maximum voltage decreased in the next 2 cycles after RB19 was first added at 1400 h. One of the possible reasons could be that some RB19 degradation intermediates were toxic to the electricity-generating bacteria, thus inhibiting the electricity production. It was found that the voltage resumed to the normal level when RB19 addition was stopped

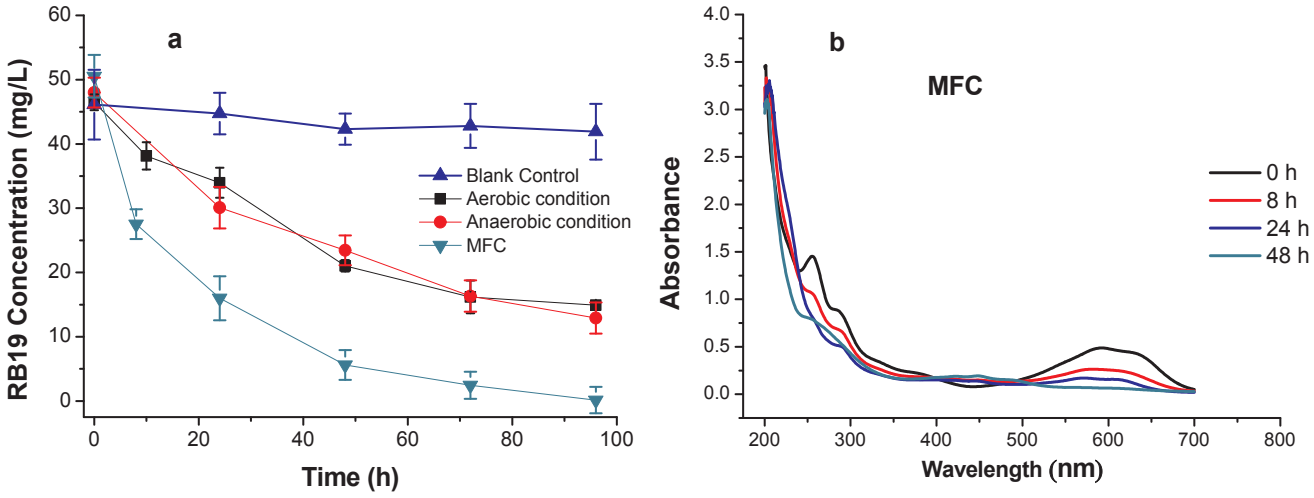

Fig. 4. (a) RB19 reduction in different treatment processes and; (b) UV–visible absorption spectra of RB19 degradation in MFC.

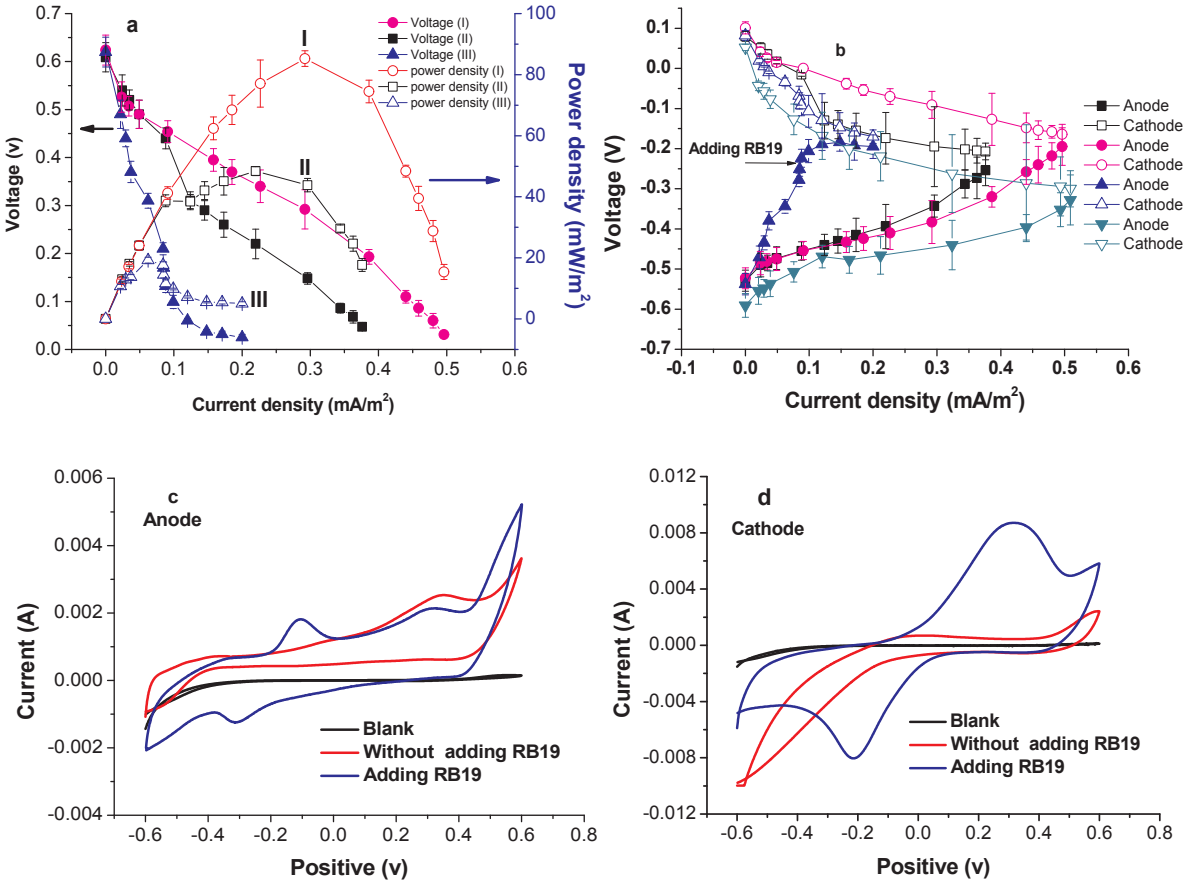

Fig. 5. CV curves of the MFC before and after the addition of RB19. (a) Before the addition of RB19 where I = exoelectrogen inoculation without RB19; II = starting period of the MFC; and III = exoelectrogen inoculation with RB19; (b) After the addition of RB19; (c) CV curve for anode; and (d) CV curve for cathode.

at 2300 h (the second red arrow in Fig. 3), which also indicated that the intermediates of RB19 degradation could inhibit the electricity-generating bacteria.

3.2. Decolorization of RB19 in the MFC

When the MFC was stable after the startup stage, the simulated wastewater containing 50 mg/L of RB19 was treated by four different decolorization processes with the dissolved oxygen (DO) concentration above 2.0 mg/L at a room temperature, which was described in Section 2.3.

The decolorization efficiency of RB19 by the MFC was monitored and compared with other processes. It was found that RB19 decolorization rate in the MFC was much higher than that in other processes (Fig. 4a). In the MFC, the RB19 degradation within 48 h already reached 89%, whereas the open circuit and aerobic condition had much lower RB19 degradation rates which were 51 and 55%, respectively. The superior decolorization efficiency of the MFC could be due to both degradation and adsorption of RB19 by the anaerobic microbes in the anode chamber while efficient electron transport in the MFC could also

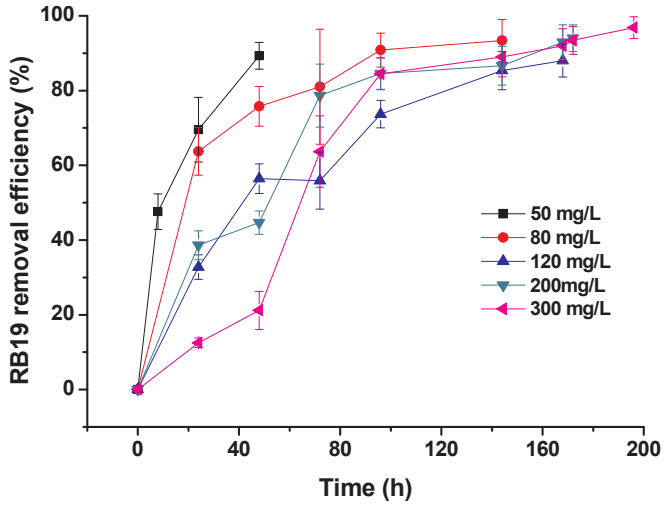

Fig. 6. Effect of the initial RB19 concentration on decolorization efficiency in the anode chamber of MFC.

promote the rapid degradation of RB19. With the extension of time to 96 h, the open loop and aerobic conditions achieved 73 and 68% of RB19 decolorization, respectively while almost 100% of RB19 was degraded in the MFC. Meanwhile, slight decrease of RB19 concentration was found in the blank control with 50 mg/L of RB19 (i.e., RB19 reduction rate within 96 h was only 9%), which could result from the adsorption of RB19 to the electrode material.

In order to further analyze the degradation intermediates of RB19 in the MFC system, the full wavelength (200–700 nm) microscopy analysis was conducted on the water samples withdrawn at 0, 8, 24, and 48 h. As shown in Fig. 4b, the absorption peaks at 590 nm were observed for the RB19 water samples. The absorption peak at 590 nm could be assigned to the hydrogen bonding between amino and hydroxyl groups of RB19, which strengthens the interaction between the lone pair and anthraquinone ring. The weak absorption bands at 310 nm and 240 nm could reflect the existence of a lone pair in the hydroxyl group and the matrix structure in RB19 (i.e., aromatic ring structure), respectively (Jenmao and Dyihwa, 2009). With the progress of decolorization, the peak at 590 nm disappears, which indicates that the conjugated structure in RB19 was destroyed. Meanwhile, the diminishing peaks at 310 and 240 nm suggest the destruction of aromatic ring structure. These results demonstrate the significant effect of MFC on the degradation of RB19 for decolorization of wastewater.

3.3. Polarization, power density and CV of the MFC

As shown in Fig. 5a–d, the stable voltage output, power density and polarization curves of the MFC varied depending on the operation phase and the presence of RB19. The initial open circuit voltage was about 0.61 V (when current = 0 A/m^2) (Fig. 5a). Without the addition of RB19, the maximum power density in the startup phase was 48.4 mW/m^2 and increased to 85.26 mW/m^2 with the extension of the acclimation process. Such a power density increase was probably due to the enrichment of electrochemically active bacteria on the anode, which promoted the electron transfer in the MFC system. However, the maximum power density sharply decreased to 19.22 mW/m^2 with the addition of RB19, which probably resulted from the increased overpotential of anode and the toxicity of RB19 against the electricity producing bacteria. The latter can impair the bacterial biofilm-forming capability (due to the weakened attachment capability) and the electron transferring efficiency. Through the comparison of polarization curves between anode and cathode, it was found that the sensitivity of voltage vs. current density was significantly increased with the addition of RB19, i.e., the slope of polarization curve increased because the anode overpotential increased with the increase of current density (Fig. 5b).

The CV has been widely used to investigate the electrochemical interaction between bacteria and the electrode surface in the MFC system (Liu et al., 2009; Rabaey et al., 2004). To reveal the difference of the electrochemical reaction at the anode before and after RB19 addition, we compared the CV characteristics of anode and cathode (Fig. 5c and d). Over the tested range of −0.6–0.6 V, the bacterium inoculation in the presence of RB19 had the strongest current response for both electrodes followed by the bacterium inoculation without RB19 and the blank control (with negligible response current) by using the same stimulating electric potential. For the anode with RB19, two pair of REDOX peaks were observed, i.e., one pair with −0.31 V of oxidation peak and 0.31 V of reduction peak, and the other pair with an oxidation peak at −0.1 V and a reduction peak at 0.1 V, while only one pair of weak REDOX peak was observed in the absence of RB19. For the cathode with RB19, only one pair of weak REDOX peak was observed in the absence of RB19, i.e., one pair with −0.2 V of oxidation peak and 0.2 V of reduction peak. Such findings indicate that RB19 can promote the electrochemical reaction on the surface of the electrodes. The group of bacteria can mediate electron transfer from the cathode electrode to oxygen directly through catalysis of the re-oxidation of redox couples (transition metals). It is essential to obtain detailed information about how these interactions work with each other in the mixed culture system.

3.4. Effect of the initial RB19 concentration on the decolorization by MFC

As shown in Fig. 6, the RB19 removal efficiency exceeded 90% with the initial RB19 concentration ranging from 50 to 300 mg/L in the anode chamber while the overall RB19 degradation rate increased with the decrease of the initial RB19 concentration. However, there seems to be a lag phase during the first 50 h when the initial RB19 is 300 mg/L, indicating a potential inhibition of RB19 on microbial activities. The dynamics of RB19 degradation process was simulated and the constants were shown in Table 2. In general, the degradation of RB19 (i.e., decolorization of wastewater) can be described by first-order kinetics (Fig. 6) and the rate constants under different initial RB19 concentrations were found to match the characteristics of the first order rate constant (Table 2).

3.5. FTIR analysis

FTIR analysis was conducted on the sludge samples withdrawn at the beginning (0 h) and the end (96 h) of RB19 decolorization in the anode chamber. As shown in Fig. 7, the peaks at 670 and 870 cm^{-1} represent the aromatic ring, and their intensities decreased significantly after 96 h, which indicates the biodegradation of RB19 in MFC. The reduction of the peak intensity around 1630 cm^{-1} reflected the stretching vibration of C═O and C═N bonds resulted from the breakdown of anthraquinone rings (Mondal, 2008). In addition, the decrease of peak intensity at 1189 cm^{-1} showed the fracture of the bond between benzene and anthraquinone rings.

In addition to aromatic ring structure, other functional groups on the benzene rings were also decomposed (Fig. 7). For example, the peak intensities at 1037/1120 and 3441 cm^{-1} (corresponding to the C–NH$_2$ and N–H bonds, respectively) diminished during the RB19 treatment.

Table 2
First order rate constants for RB19 decolorization in MFC under different initial concentrations.

Initial RB19 concentration (mg/L)	50	80	120	200	300
k_{app} (mg/L·h)	0.0444	0.0229	0.0129	0.0154	0.0176
R^2	0.983	0.947	0.972	0.951	0.963

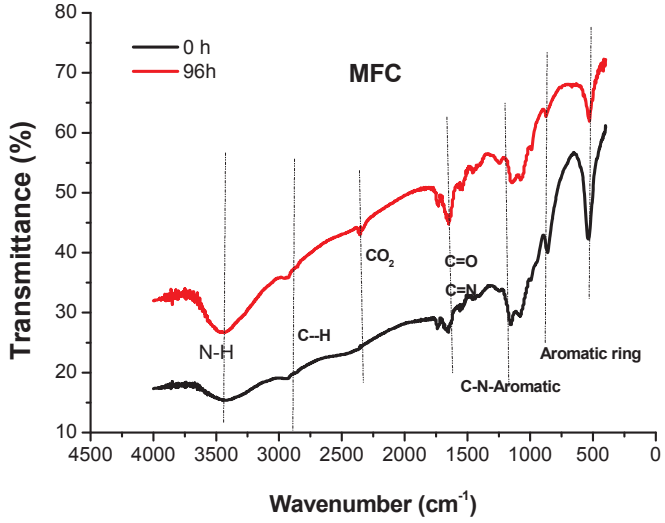

Fig. 7. FTIR spectra analysis of the RB19 in the MFC.

The absorbance bands at 2924 and 2853 cm^{-1} represented the symmetric and asymmetric C–H bonds of $–CH_2$, respectively, which could be derived from the degradation of $–SO_2CH_2CH_2OSO_3Na$. In addition, a new characteristic CO_2 absorption peak emerged at about 2340 cm^{-1} during the degradation of RB19, which is similar to the result of RB19 degradation with ozone (Dignac et al., 2000).

3.6. Microbial community in the MFC

After 16S rRNA gene sequencing was done, the sequence reads underwent a series of quality filtration to trim and/or remove poor-quality data and were clustered into OTU sat a 97% similarity threshold using UPARSE (version 7.1, http://drive5.com/uparse/). Chimeric sequences were identified and removed using UCHIME. The taxonomy of each 16S rRNA gene sequence was analyzed by using RDP Classifier (http://rdp.cme.msu.edu/) against the silva (SSU115) 16S rRNA database using confidence threshold of 70%. As shown in Table 3, the coverage for all sludge samples was over 0.999.

In general, the indexes of ace and chao indicate the microbial community richness (i.e., higher ace and chao indexes mean higher richness of the microbial community), while the Shannon and simpson indexes reflect the diversity of microbial community (i.e., higher Shannon index mean higher diversity of microbial community, while the indication of simpson index is opposite to that of Shannon index). As shown in Table 3, both ace and chao indexes of sludge A2 and A3 were lower than those of A1, indicating that acclimation process reduced the richness of microbial community and enriched the dominant microorganisms. It was also found that the Shannon index gradually decreased and the Simpson index increased to some extent, suggesting that the diversity of microbial community was reduced during acclimation and that successive acclimation approach was effective for the enrichment of dominant microorganisms.

Table 3
Sequence reads, OTUs, coverage, and the indexes of richness and diversity of the sludge samples.

Sample ID	Number of sequence reads	0.97 similarity					
		OTU	ace	chao	coverage	shannon	simpson
A1	56,024	487	494	492	0.999,732	4.82	0.0199
A2	81,345	303	373	389	0.999,127	3.45	0.0644
A3	75,428	242	288	291	0.999,470	3.75	0.0468
A4	75,781	136	152	153	0.999,762	1.58	0.5187
A5	66,982	297	335	334	0.999,268	2.82	0.1603

Note: A1 = original anaerobic sludge, A2 = acclimated anaerobic sludge for RB19 decolorization, A3 = acclimated aerobic sludge for RB19 decolorization, A4 = the sludge from the anode chamber of the MFC without the addition of RB19, and A5 = the sludge from the anode chamber of the MFC with RB19.

The relative abundance is defined as the percentage of the same taxon to the corresponding total sequences for each sample. As shown in Fig. 8, bacteria in all sludge samples can be classified into 19 (including others) phyla which consisted of the total of 358 genera including 100 unclassified genera with no rank (shown as others). *Proteobacteria* were the major bacteria with the highest relative abundance of 23.1–83.87% depending on the sludge, followed by *Bacteroidetes*, *Actinobacteria*, *Firmicutes*, and *Clostridia* in that order. The dominant functioning bacteria with the relative abundance over 1% at the genus level are listed in Table 4. In the original sludge A1, the dominant bacteria were *Citrobacter* (6.45%), *Thiobacillus* (5.91%) and *Thioclava* (1.77%). In sludge A2, the dominant bacteria became *Corynebacterium* (17.6%), *Arcobacter* (10.6%), *Desulfovibrio* (4.4%), and *Geobacter* (1.1%). *Desulfovibrio* was reported to be able to decolor various azo dyes (Gilcreas, 1995). The A3, an aerobic sludge, consisted of *Stappia* (7.27%), *Thauera* (6.97%), *Azoarcus* (3.56%), *Hydrogenophaga* (2%), and *Nitrosomonas* (3.56%) as dominant genera. *Thaueragenus* was recognized to function in aromatic pollutant degradation and denitrification (Kumru et al., 2012), and it is a common genus found in many wastewater treatment plants in the processes of nitrification and dichlorination (Feng et al., 2015; Yu et al., 2016).

In the absence of RB19, the sludge A4 from MFC mainly contains exoelectrogens, such as *Vibrio* (71.1%) and *Shewanella* (1.79%) in addition to *Arcobacter* (2.9%) and *Thioclava* (1.91%) which usually use acetate as an electron donor in the anode chamber of MFC (Watson and Logan, 2010). When the RB19 was added to the anode chamber of the MFC, the microbial community compositions were significantly altered, i.e., the microbial community of the sludge A5 was dominated by the genera of *Arcobacter* (34.05%), *Thioclava* (18.49%), *Vibrio* (5.7%), *Desulfovibrio* (1.74%), *Azoarcus* (1.16%), and *Pseudomonas* (2.24%). It was reported that *Pseudomonas* and *Desulfovibrio* genera can decolor various types of azo dyes (Saratale et al., 2011). For example, the *Pseudomonas* genus has been extensively used to treat numerous azo and other industrial dyes, including Red BLI, Reactive Red 2, Red HE7B, Reactive Blue 172, Reactive Red 22, and Orange I/II, etc. Through the high-throughput 16S rRNA sequencing, the aforementioned genera can be generally classified into two groups based on their specific functions such as electrochemically active and dye-decoloring bacteria (Table 4). The first group includes *Vibrio, Arcobacter, Corynebacterium, Stappia, Desulfovibrio, Citrobacter, Pseudomonas, Shewanella*, and *Stenotrophomonas*. The second group includes *Thiobacillus* (Gabby and L, 2014; Wang et al., 2011), *Pseudomonas* (Bhatt et al., 2005), *Shewanella* (Xu et al., 2007), and *Bacillus* (Kolekar et al., 2008). Such results further indicate that the sludge acclimation is an effective technique to enrich bacteria for RB19 degradation with electricity production.

4. Conclusions

MFC is much more efficient than the traditional anaerobic and aerobic techniques on the decolorization of RB19. The investigation on the electrochemical CV of the MFC indicated that RB19 redox reaction occurred on the anode surface and competed for the electrons generated in the system, leading to significant decrease of power density of the MFC in the presence of RB19. The degradation of RB19 in the MFC follows first order kinetics. The high-throughput 16S rRNA sequencing revealed that there were two major functioning microbial communities in the MFC system such as electricity-producing and RB19-degrading bacteria. The genera including *Vibrio*, *Arcobacter*, *Corynebacterium*, *Stappia*, *Desulfovibrio*, *Citrobacter*, *Pseudomonas*, *Shewanella*, and *Stenotrophomonas* were believed to produce electricity while the genera of *Thiobacillus*, *Pseudomonas*, *Shewanella*, and *Bacillus*were were most likely responsible for RB19 degradation. The interactions among these

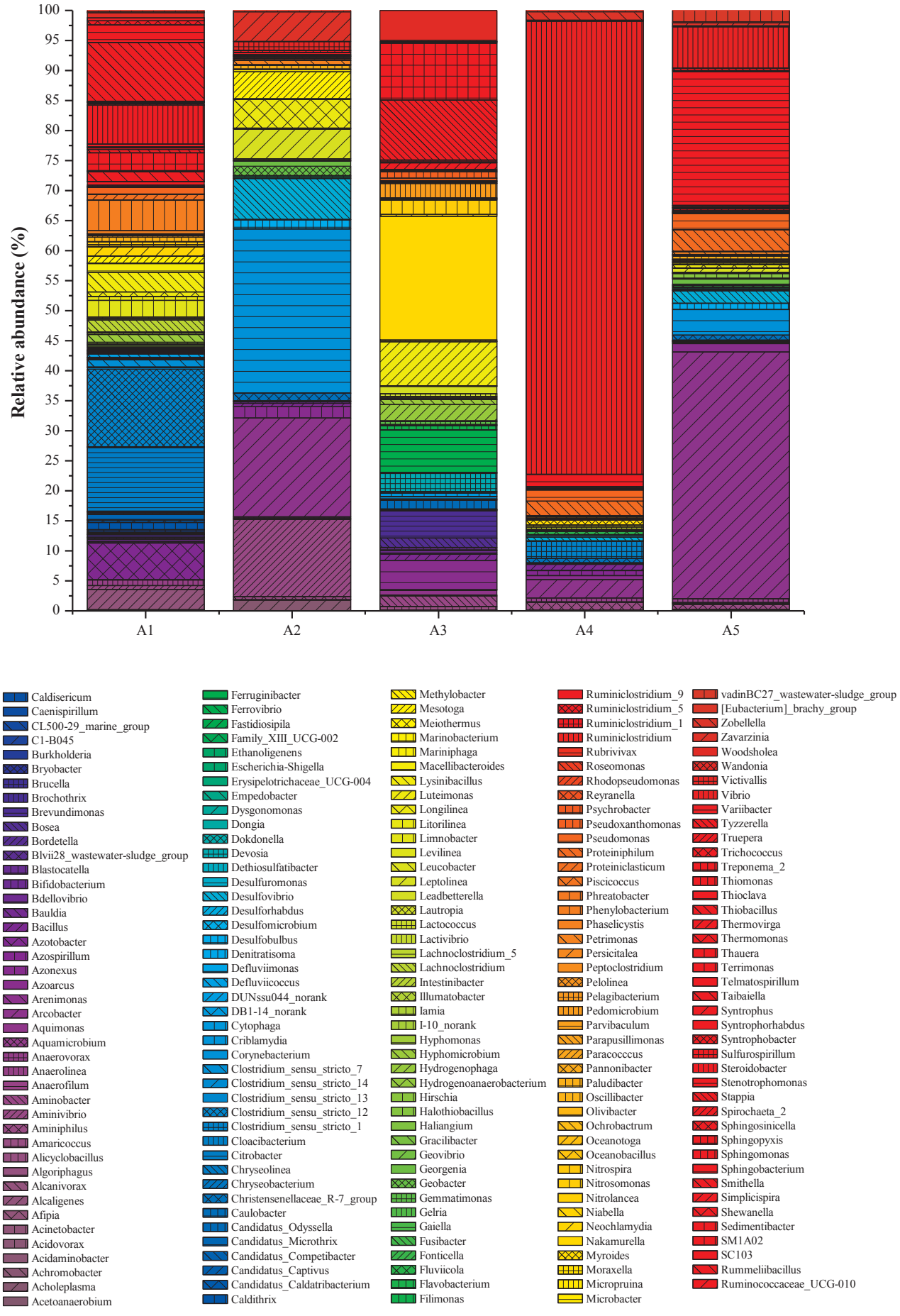

(caption on next page)

Fig. 8. Microbial diversity of five sludge samples assessed with high-throughput 16S rRNA.

Table 4
Classification of the five sludge samples.

No.	Phylum	Class	Family	Genus	Sludge				
					A1	A2	A3	A4	A5
1	*Proteobacteria*	*Gammaproteobacteria*	*Vibrionaceae*	*Vibrio*	0	0	0.02	71.7	5.7
2	*Proteobacteria*	*Epsilonproteobacteria*	*Campylobacteraceae*	*Arcobacter*	0	10.6	0.001	2.9	34.05
3	*Actinobacteria*	*Actinobacteria*	*Corynebacteriaceae*	*Corynebacterium*	0.019	17.6	0.3	0.002	3.5
4	*Proteobacteria*	*Alphaproteobacteria*	*Rhodobacteraceae*	*Thioclava*	1.77	0.24	0.008	1.91	18.49
5	*Proteobacteria*	*Alphaproteobacteria*	*Rhodobacteraceae*	*Stappia*	0	0.001	7.27	0.1	0.2
6	*Proteobacteria*	*Betaproteobacteria*	*Rhodocyclaceae*	*Thauera*	0.007	0.006	6.97	0.001	0
7	*Proteobacteria*	*Deltaproteobacteria*	*Desulfovibrionaceae*	*Desulfovibrio*	0	4.4	0	0.62	1.74
8	*Proteobacteria*	*Betaproteobacteria*	*Rhodocyclaceae*	*Azoarcus*	0	0.01	3.56	0.64	1.16
9	*Bacteroidetes*	*Bacteroidia*	*Porphyromonadaceae*	*Proteiniphilum*	0.02	0.16	0.005	2.28	2.97
10	*Proteobacteria*	*Gammaproteobacteria*	*Enterobacteriaceae*	*Citrobacter*	6.45	0.03	0.001	0.004	0.004
11	*Proteobacteria*	*Gammaproteobacteria*	*Pseudomonadaceae*	*Pseudomonas*	0.69	0.09	0.32	1.79	2.24
12	*Proteobacteria*	*Betaproteobacteria*	*Hydrogenophilaceae*	*Thiobacillus*	5.91	0.007	0	0	0.03
13	*Proteobacteria*	*Betaproteobacteria*	*Nitrosomonadaceae*	*Nitrosomonas*	0.19	0	1.76	0	0
14	*Proteobacteria*	*Deltaproteobacteria*	*Geobacteraceae*	*Geobacter*	0.002	1.01	0	0	0
15	*Proteobacteria*	*Gammaproteobacteria*	*Moraxellaceae*	*Acinetobacter*	0	0.6	0.8	1.4	0.67
16	*Proteobacteria*	*Betaproteobacteria*	*Comamonadaceae*	*Hydrogenophaga*	0.15	0.001	2.0	0.01	0.01
17	*Proteobacteria*	*Gammaproteobacteria*	*Shewanellaceae*	*Shewanella*	0.69	0.09	0.3	1.79	2.24
18	*Firmicutes*	*Bacilli*	*Bacillaceae*	*Bacillus*	0.04	0.36	0.76	0.95	0.12
19	*Proteobacteria*	*Gammaproteobacteria*	*Xanthomonadaceae*	*Stenotrophomonas*	0.28	0.019	0.04	0.087	0.14

microorganisms resulted in highly efficient RB19 decolorization and electricity generation in the MFC, and the culture acclimation was important to achieve successful RB19 degradation.

Declarations of interest

None.

Acknowledgements

This work was supported by the National Natural Science Foundation of China (Grant No.:20076037, 2014) and Principal fund of Xiamen University (Grant No.:20720170034, 2017).

References

An, B.M., Heo, Y., Maitlo, H.A., Park, J.Y., 2016. Scaled-up dual anode/cathode microbial fuel cell stack for actual ethanolamine wastewater treatment. Bioresour. Technol. 210, 68–73.

Asghar, A., Abdul Aziz, A.R., Mohd, A.W.D.W., 2015a. Advanced oxidation processes for in-situ production of hydrogen peroxide/hydroxyl radical for textile wastewater treatment: a review. J. Clean. Prod. 87, 826–838.

Asghar, A., Abdul Raman, A.A., Daud, W.M.A.W., 2015b. Recent advances, challenges and prospects of in situ production of hydrogen peroxide for textile wastewater treatment in microbial fuel cells. J. Chem. Technol. Biotechnol. 89, 1466–1480.

Bali, U., Çatalkaya, E.S., engül, F., 2004. Photodegradation of reactive black 5, directred 28 and direct yellow 12 using UV, UV/H_2O_2 and UV/H_2O_2/Fe^{2+}: a comparative study. J. Hazard Mater. 114, 159–166.

Basturk, E., Karatas, M., 2014. Decolorization of antraquinone dye reactive blue 181 solution by UV/H_2O_2 process. J. Photochem. Photobiol., A 299, 67–72.

Beydilli, I., Pavlostathis, S.G., Tincher, W.C., 2000. Biological decolorization of the azo dye Reactive Red 2 under various oxidation-reduction conditions. Water Environ. Res. 72, 698.

Bhatt, N., Patel, K.C., Keharia, H., Madamwar, D., 2005. Decolorization of diazo-dye reactive blue 172 by Pseudomonas aeruginosa NBAR12. J. Basic Microbiol. 45, 407–418.

Brillas, E., Martínez-Huitle, C.A., 2015. Decontamination of wastewaters containing synthetic organic dyes by electrochemical methods. An updated review. Appl. Catal. B Environ. 166–167, 603–643.

Buscio, V., Marín, M.J., Crespi, M., Gutiérrez-Bouzán, C., 2015. Reuse of textile wastewater after homogenization-decantation treatment coupled to PVDF ultrafiltration membranes. Chem. Eng. J. 265, 122–128.

Chen, B.Y., Hsueh, C.C., Liu, S.Q., Hung, J.Y., Qiao, Y., Yueh, P.L., Wang, Y.M., 2013. Unveiling characteristics of dye-bearing microbial fuel cells for energy and materials recycling: redox mediators. Int. J. Hydrogen Energy 38, 15598–15605.

Dignac, M.F., Derenne, S., Ginestet, P., Bruchet, A., Knicker, H., Largeau, C., 2000. Determination of structure and origin of refractory organic matter in bio-epurated wastewater via spectroscopic methods. Comparison of conventional and ozonation treatments. Environ. Sci. Technol. 34, 3389–3394.

Du, Z., Li, H., Gu, T., 2007. A state of the art review on microbial fuel cells: a promising technology for wastewater treatment and bioenergy. Biotechnol. Adv. 25, 464.

Feng, C., Huang, L., Yu, H., Yi, X., Wei, C., 2015. Simultaneous phenol removal, nitrification and denitrification using microbial fuel cell technology. Water Res. 76, 160.

Fontenot, E.J., Beydilli, M.I., Lee, Y.H., Pavlostathis, S.G., 2002. Kinetics and inhibition during the decolorization of reactive anthraquinone dyes under methanogenic conditions. Water Sci. Technol. 10, 105.

Gabby, T.C.E., L, K., 2014. Review of reductive leaching of iron by anaerobic bacteria. Min. Proc. Ext. Met. Rev. 35, 75–105.

Ge, Y., Wei, B., Wang, S., Guo, Z., Xu, X., 2015. Optimization of anthraquinone dyes decolorization conditions with response surface methodology by Aspergillus. Korean Chem. Eng. Res. 53, 327–332.

Gilcreas, F.W., 1995. Standard methods for the examination of water and waste water. Am. J. Public Health Nation's Health 4, 387–388.

Habibi, M.H., Hassanzadeh, A., Mahdavi, S., 2005. The effect of operational parameters on the photocatalytic degradation of three textile azo dyes in aqueous TiO_2 suspensions. J. Photochem. Photobiol. A Chem. 172, 89–96.

Imran, M., Crowley, D.E., Khalid, A., Hussain, S., Mumtaz, M.W., Arshad, M., 2015. Microbial biotechnology for decolorization of textile wastewaters. Rev. Environ. Sci. Biotechnol. 14, 73–92.

Jenmao, F., Dyihwa, T., 2009. Degradation of anthraquinone dye C.I. Reactive Blue 19 in aqueous solution by ozonation. Chemosphere 77, 214–221.

Jian, S., Hu, Y.Y., Zhe, B., Cao, Y.Q., 2009. Simultaneous decolorization of azo dye and bioelectricity generation using a microfiltration membrane air-cathode single-chamber microbial fuel cell. Bioresour. Technol. 100, 3185.

Jung, S., Regan, J.M., 2007. Comparison of anode bacterial communities and performance in microbial fuel cells with different electron donors. Appl. Microbiol. Biotechnol. 77, 393–402.

Kolekar, Y., Pawar, S., Gawai, K., Lokhande, P., Shouche, Y., Kodam, K., 2008. Decolorization and degradation of Disperse Blue 79 and Acid Orange 10, by Bacillus fusiformis KMK5 isolated from the textile dye contaminated soil. Bioresour. Technol. 99, 8999–9003.

Kumru, M., Eren, H., Catal, T., Bermek, H., Akarsubaşi, A.T., 2012. Study of azo dye decolorization and determination of cathode microorganism profile in air-cathode microbial fuel cells. Environ. Technol. 33, 2167–2175.

Liu, L., Li, F.B., Feng, C.H., Li, X.Z., 2009. Microbial fuel cell with an azo-dye-feeding cathode. Appl. Microbiol. Biotechnol. 85, 175.

Logan, B.E., Wallack, M.J., Kim, K.Y., He, W., Feng, Y., Saikaly, P.E., 2015. Assessment of microbial fuel cell configurations and power densities. Environ. Sci. Technol. Lett. 2, 150803121308002.

Mondal, S., 2008. Methods of dye removal from dye house effluent: an overview. Environ. Eng. Sci. 25, 383–396.

Ning, X.A., Liang, J.Y., Li, R.J., Hong, Z., Wang, Y.J., Chang, K.L., Zhang, Y.P., Yang, Z.Y., 2015. Aromatic amine contents, component distributions and risk assessment in sludge from 10 textile-dyeing plants. Chemosphere 134, 367.

O'Neill, C., Hawkes, F.R., Hawkes, D.L., Lourenço, N.D., Pinheiro, H.M., Delée, W., 2015. Colour in textile effluents-sources, measurement, discharge consents and simulation: a review. J. Chem. Technol. Biotechnol. 74, 1009–1018.

Penteado, E.D., Fernandez-Marchante, C.M., Zaiat, M., Cañizares, P., Gonzalez, E.R.,

Rodrigo, M.A., 2016. Influence of sludge age on the performance of MFC treating winery wastewater. Chemosphere 151, 163.
Rabaey, K., Boon, N., Siciliano, S.D., Verhaege, M., Verstraete, W., 2004. Biofuel cells select for microbial consortia that self-mediate electron transfer. Appl. Environ. Microbiol. 70, 5373–5382.
Santos, S.C., Boaventura, R.A., 2015. Treatment of a simulated textile wastewater in a sequencing batch reactor (SBR) with addition of a low-cost adsorbent. J. Hazard Mater. 291, 74–82.
Saratale, R.G., Saratale, G.D., Chang, J.S., Govindwar, S.P., 2011. Bacterial decolorization and degradation of azo dyes: a review. J. Taiwan Inst. Chem. E. 42, 138–157.
Shamsnejati, S., Chaibakhsh, N., Pendashteh, A.R., Hayeripour, S., 2015. Mucilaginous seed of Ocimum basilicum as a natural coagulant for textile wastewater treatment. Ind. Crops Prod. 69, 40–47.
Skoog, D.A., Holler, F.J., Crouch, S.R., 1998. Principles of Instrumental Analysis Sixth Edition, vol. 18. pp. 45.
Soares, O.S.G., Orfao, J.J., Portela, D., Vieira, A., Pereira, M.F.R., 2006. Ozonation of textile effluents and dye solutions under continuous operation: influence of operating parameters. J. Hazard Mater. 137, 1664–1673.
Sun, J.H., Sun, S.P., Wang, G.L., Qiao, L.P., 2007. Degradation of azo dye Amido black 10B in aqueous solution by Fenton oxidation process. Dyes Pigments 74, 647–652.
Sun, J., Bi, Z., Hou, B., Cao, Y.Q., Hu, Y.Y., 2011. Further treatment of decolorization liquid of azo dye coupled with increased power production using microbial fuel cell equipped with an aerobic biocathode. Water Res. 45, 283.
Wang, H.T., Li, Q.B., Lu, Y.H., et al., 2007. Performance of batch-operated combined hydrolytic-aerobic biofilm process in treating anthraquinone reactive dye wastewater. Environ. Eng. Sci. 24, 483–488.
Wang, X., Yao, Z., Wang, J., Guo, W., Li, G., 2008. Degradation of reactive brilliant red in aqueous solution by ultrasonic cavitation. Ultrason. Sonochemistry 15, 43–48.
Wang, H.M., Min, X.B., Chai, L.Y., Shu, Y.D., 2011. Biological preparation and application of poly-ferric sulfate flocculant. T. Nonferr. Metal. Soc. 21, 2542–2547.
Watson, V.J., Logan, B.E., 2010. Power production in MFCs inoculated with Shewanella oneidensis MR-1 or mixed cultures. Biotechnol. Bioeng. 105, 489.
Xu, M., Guo, J., Sun, G., 2007. Biodegradation of textile azo dye by Shewanella decolorationis S12 under microaerophilic conditions. Appl. Microbiol. Biotechnol. 76, 719–726.
Yu, H., Feng, C., Liu, X., Yi, X., Ren, Y., Wei, C., 2016. Enhanced anaerobic dechlorination of polychlorinated biphenyl in sediments by bioanode stimulation. Environ. Pollut. 211, 81–89.
Zhou, F., Song, H.L., Ning, C., Li, X.N., 2015. Electricity production from Azo dye wastewater using a microbial fuel cell coupled constructed wetland operating under different operating conditions. Biosens. Bioelectron. 68, 135–141.